Biophysical Chemistry 160 (2012) 62–68

Contents lists available at SciVerse ScienceDirect

Biophysical Chemistry

journal homepage: http://www.elsevier.com/locate/biophyschem

Properties of compatible solutes in aqueous solution

Jens Smiatek [a,*], Rakesh Kumar Harishchandra [b], Oliver Rubner [a], Hans-Joachim Galla [b], Andreas Heuer [a]

[a] Institut für Physikalische Chemie, Westfälische Wilhelms-Universität Münster, D-48149 Münster, Germany
[b] Institut für Biochemie, Westfälische Wilhelms-Universität Münster, D-48149 Münster, Germany

HIGHLIGHTS

- Investigation of solvent structure around compatible solutes via Molecular Dynamics simulations.
- Numerical study validates strong hygroscopic effect of ectoines.
- Long range influence on water structure is indicated.
- Independent on salt concentration.
- Qualitative agreement with presented experiments.

GRAPHICAL ABSTRACT

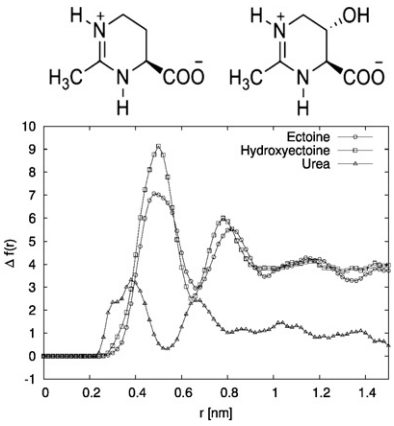

ARTICLE INFO

Article history:
Received 18 July 2011
Received in revised form 19 September 2011
Accepted 20 September 2011
Available online 29 September 2011

Keywords:
Compatible solute
Molecular Dynamics simulation
Aqueous solution

ABSTRACT

We have performed Molecular Dynamics simulations of ectoine, hydroxyectoine and urea in explicit solvent. Special attention has been spent on the local surrounding structure of water molecules. Our results indicate that ectoine and hydroxyectoine are able to accumulate more water molecules than urea by a pronounced ordering due to hydrogen bonds. We have validated that the charging of the molecules is of main importance resulting in a well defined hydration sphere. The influence of a varying salt concentration is also investigated. Finally we present experimental results of a DPPC monolayer phase transition that validate our numerical findings.

1. Introduction

Extremolytes are natural compounds which are synthesized by extremophilic microorganisms. Chemically they are organic osmolytes which are build of amino acids, betain, sugar and heteroside derivatives [1]. Thus the name extremolyte is a coinage: organic osmolytes which are synthesized by extremophilic microorganisms. The presence of these molecules allows microorganisms to resist extreme living conditions like drastic temperature variations and high salinity [1,2]. Interestingly, these solutes are biologically inert and accumulate at high concentration in the cytoplasm without interfering with the overall cellular functions; hence they are called *compatible solute* [3].

Long-known compatible solutes are ectoine and hydroxyectoine occurring in anaerobic chemoheterotrophic and halophilic/halotolerant bacteria [3–6]. The main characteristics are given by a low molecular weight and strong water binding properties. It was indicated by experiments [7,8] and ab initio molecular orbital studies [9] in aqueous

* Corresponding author.
E-mail address: jens.smiatek@uni-muenster.de (J. Smiatek).

0301-4622/$ – see front matter © 2011 Elsevier B.V. All rights reserved.
doi:10.1016/j.bpc.2011.09.007

solution that the zwitterionic structure is more stable than the neutral form. The structural formulae of these molecules are presented in Fig. 1.

Over the last years the stupendous characteristics of these small molecules have succeeded to explore a novel application area in dermatological industry. Long used hygroscopic molecules like urea have been systematically replaced by extremolytes in a stepwise manner [10]. Specifically ectoine and hydroxyectoine have been used as cell protectant in skin care [2,10] due to their accessibility of large scale production [1,4–6].

Further biological importance is given by the stabilization of proteins in presence of compatible solutes [11,12]. The reason for this protective behavior can be explained by a complex interplay between all species. Several studies have investigated this mechanism in detail [13–19]. Most of the theories prefer an indirect mechanism in which the compatible solute does not directly interact with the macromolecule. An important theory in this context is the preferential exclusion model [13–16] which states that the appearance of the co-solvent leads to thermodynamic interactions with the protein [16]. Due to these interactions, the protein repels the co-solvent from its surface to the bulk region. Thus the concentration of the co-solvent is lower in close vicinity to the protein whereas its bulk value is increased. This can only be accomplished by the addition of excess water molecules to the proteins surface which results in a preferential hydration of the macromolecule [16]. The excess water molecules finally conserve the native form such that unfolding becomes less favorable which is realized by an increase of the melting temperature [13,20–23].

Numerical investigations have further identified a significant decrease in the activity coefficient of water in presence of hydroxyectoine and ectoine [24]. In addition it was found that compatible solutes fluidize lipid monolayers by acting along the line tension [25,26]. Direct interactions have to be also taken into account as it was shown for high concentrations of hydroxyectoine [26] which again emphasizes the indirect mechanism described above. This effect has been shown as advantageous for cell membranes due to an acceleration of repair mechanisms and signaling processes [27]. To summarize, the presence of compatible solutes allows proteins as well as cell membranes to resist environmental stress and to support the regeneration and the protection of the native structure.

In this paper we focus on the hygroscopic behavior of ectoine and hydroxyectoine in comparison to urea. Special emphasis is spent on the structural ordering of the local water environment. These results are important for a further understanding of the mechanisms of compatible solutes and their corresponding functionality.

We have performed Molecular Dynamics simulations where the specific influence of extremolytes on the molecular structure of water is investigated via radial distribution functions. The influence of a varying salt concentration was also investigated. Our conclusions about the structural alteration of the local solvent environment are supported by experimental results of a DPPC monolayer phase transition. It has been recently discussed [26] that compatible solutes interact with the membrane via a solvent-mediated mechanism. Hence, we will show that the relative influence in the ordering of water by a compatible solute is directly reflected in the broadening mechanism of a liquid expanded/liquid condensed phase transition. It has to be noticed that we do not aim to numerically investigate this mechanism in detail. The experimental results serve as a validation for the perturbation exerted by different compatible solutes on the local water environment as it has been found in our simulations.

In addition we discuss the hygroscopic properties of the different molecules in atomistic detail. Our results allow to interpret the numerical findings of a recent publication [21] and validate the experimental consensus that extremolytes are more appropriate for water binding than other compatible solutes [1,2,10,25]. We will show that the length scale of solvent perturbation is identical to the distance between a protein and a compatible solute in agreement to Ref. [21].

The paper is organized as follows. In the next sections we present the theoretical background and the numerical and experimental details. The results and the discussion are presented in the fourth section and we finally conclude with a brief summary in the fifth section.

2. Numerical details

Our simulations have been performed in explicit SPC/E water model solvent [28] with the software package GROMACS [29–31] and variations of the force field GROMOS96 [32]. The initial chemical structure was created via the SMILES language [33,34]. The topology file with the essential molecular dynamics parameters has been derived by the usage of the PRODRG server [35]. The structure and the charges of ectoine, hydroxyectoine and urea have been refined and calculated by the software package TURBOMOLE 6.1 [36]. By applying Møller–Plesset perturbation theory (RI-MP2) with the TZVPP basis set [37,38], we performed a geometry optimization in combination with the COSMO solvent model [39,40]. We found that the zwitterionic forms of ectoine and hydroxyectoine are 10.81 kcal/mol and 12.35 kcal/mol, respectively, more stable than the neutral counterparts. Hence we neglect all Molecular Dynamics simulations regarding neutral ectoine and neutral hydroxyectoine.

After geometry optimization and calculation of the atomistic properties, we transferred the corresponding values for the equilibrium parameters of the bond length, the partial charges and the bond angles to the PRODRG topology file. The modified PRODRG file, where all other atomistic parameters as given by the GROMOS96 force field [32] were left unchanged, was finally used for the classical Molecular Dynamics simulations.

The atomistic simulations have been carried out in a cubic simulation box with periodic boundary conditions. The box for ectoine was $(4.5342\times4.5342\times4.5342)\,\mathrm{nm}^3$ filled with 3077 SPC/E water molecules. Hydroxyectoine has been simulated within a box size of $(4.6153\times4.6153\times4.6153)\,\mathrm{nm}^3$ and 3261 water molecules. The results for urea have been derived in a box of $(4.4015\times4.4015\times4.4015)\,\mathrm{nm}^3$ with 2803 water molecules. The solvent density was nearly identical for all simulations.

Electrostatic interactions have been calculated by the Particle Mesh Ewald sum [41] in an electroneutral system. Varying salt concentrations have been achieved by replacing water molecules by the analog number of chloride and sodium ions.

The time step was $\delta t = 2$ fs and the temperature was kept constant at 300 K by a Nose-Hoover thermostat [42]. All bonds have been constrained by the LINCS algorithm [43]. After minimizing the energy, we performed 100 ps of equilibration followed by a 10 ns simulation sampling run.

The structure of the solution has been investigated by the radial distribution function [44]

$$g_{AB}(r) = \frac{\langle \rho_B(r) \rangle}{\langle \rho_B \rangle} \tag{1}$$

which gives the probability of finding a molecule B around molecule A compared to the ideal gas description, where $<\rho_B(r)>$ denotes the particle density of type B at a distance r around particle A and $<\rho_B>$ describes the average particle density of B within a distance d around A.

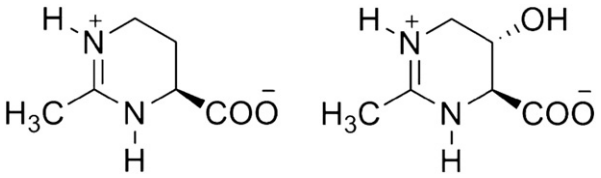

Fig. 1. Structural formulae of ectoine (left) and hydroxyectoine (right).

The cumulative particle number function is given by

$$f_{AB}(r) = 4\pi\langle\rho_B\rangle\int_0^d r^2\, dr\, g_{AB}(r) \quad (2)$$

and yields an estimate for the number of molecules within the distance d. A further important quantity is the number of present hydrogen bonds n_{HB}. Division of this value by the total solvent accessible surface area σ_t gives

$$\rho_{HB} = \left\langle \frac{n_{HB}(t)}{\sigma_t(t)} \right\rangle \quad (3)$$

the hydrogen bond density [21] that counts the average number of hydrogen bonds per unit surface area. The solvent accessible surface area is calculated by the sum of spheres centered at the atoms of the studied molecule, such that a spherical solvent molecule can be placed in closest distance and in agreement to van-der-Waals interactions by following the constraint that other atoms are not penetrated [45]. A hydrogen bond is present, if the distance between the interacting atoms is closer than 0.35 nm and the interaction angle is not larger than 30°.

To compare the molecules we have calculated the solvent accessible hydrophilic surface area σ_h [45] as given for the hydrophilic atoms of the molecule, which is divided by the total solvent accessible surface area resulting in the ratio r_σ.

The influence of the charged functional groups can be estimated by conducting simulations where the partial charges of the compatible solutes have been set to zero such that the complete molecule was uncharged. The number of hydrogen bonds calculated in these simulations was subtracted from the average number of hydrogen bonds n_{HB} present at the charged molecules resulting in the net average number of hydrogen bonds n_{HB}^c. The difference of the charged and uncharged molecules cumulative radial distribution function of water molecules is given by $\Delta f(r) = f_{AB}(r) - f_{AB}^{uc}(r)$.

3. Experimental details

The lipid DPPC (1,2-dipalmitoyl-sn-glycero-3-phosphocholine) was purchased from Avanti Polar Lipids Inc. (Alabaster, AL). 2-(4,4-Difluoro-5-methyl-4-bora-3a,4a-diaza-s-indacene-3-dodecanoyl)-1-hexadecanoyl-sn-glycero-3-phosphocholine (β-BODIPY® 500/510 C_{12}-HPC, BODIPY-PC) was obtained from Molecular Probes (Eugene, OR). The DPPC was dissolved in chloroform/methanol solution (1:1, v/v). Chloroform and methanol were high pressure liquid chromatography grade and purchased from Sigma-Aldrich (Steinheim, Germany) and Merck (Darmstadt, Germany), respectively. Urea was purchased from Roth Chemie GmbH (Karlsruhe, Germany). Ectoine ((S)-2-methyl-1,4,5,6-tetrahydropyrimidine-4-carboxylic acid) and hydroxyectoine ((4S,5S)-2-methyl-5-hydroxy-1,4,5,6-tetrahydropyrimidine-4-carboxylic acid) were obtained from Bitop AG (Witten, Germany). Water was purified and deionized by a multicartridge system (MilliPore, Billerica, MA) and had a resistivity >18 M Ωm.

Domain structures of DPPC doped with 0.5 mol% BODIPY-PC were visualized by means of video-enhanced epi-fluorescence microscope (Olympus STM5-MJS, Olympus, Hamburg, Germany) equipped with a xyz-stage and connected to a CCD camera (Hamamatsu, Herrsching, Germany). The analytical Wilhelmy film balance (Riegler and Kirstein, Mainz, Germany) with an operational area of 144 cm^2 was placed on the xyz-stage of the microscope. All measurements were performed on the subphase containing pure water, ectoine, hydroxyectoine or urea, at 20 °C. The DPPC solution from an organic solvent was spread on the subphase and left for 10–15 min for the solvent to evaporate followed by compressing the monolayer at a rate of 2.9 cm^2/min.

The images were captured by stopping the barrier and equilibrating the monolayer for few minutes at desired surface pressures.

4. Results and discussion

To understand the influence of compatible solutes on an aqueous solution, we analyzed the configuration of water molecules around ectoine, hydroxyectoine and urea and studied several static properties.

The results are presented in Table 1. It is obvious that the ectoines are different compared to urea in their ratio of the hydrophilic to the total surface area r_σ. The hydrophilic surface area σ_h shows a slight increase in the order of urea, ectoine and hydroxyectoine. The net number of hydrogen bonds n_{HB}^c is larger for ectoine and hydroxyectoine. The values for n_{HB}^c are slightly smaller than n_{HB} for all molecules. The hydrogen bond densities for the total surface areas ρ_{HB} are in the range of 2.75–3.39 nm^{-2}. Hence compared to the values of n_{HB}, it is obvious that the number of hydrogen bonds constantly grows with the total surface area. Thus the larger number of hydrogen bonds for ectoine and hydroxyectoine can be partly related to a simple size effect.

To investigate the characteristics of the water binding properties in more detail, we further studied the effects of the functional groups on the corresponding number of present hydrogen bonds. Therefore we identified the polar groups in each molecule and numbered them by R1–R7 (Fig. 2). The data together with the corresponding average lifetimes are displayed in Table 2 with the notation given in Fig. 2.

Most of the hydrogen bonds are present at the carboxylic group (R1) of the extremolytes. An increased value of hydrogen bonds for urea is induced by the oxygen group (R7). The lifetimes for a hydrogen bond with urea (R7) and for the extremolytes (R1) are comparable. The average lifetime of hydrogen bonds between water molecules has been found to be around 2.72 ps which indicates that the values displayed in Table 2 are induced by well coordinated and localized water molecules. Regarding the results for the hydrogen bond density ρ_{HB} and the number of hydrogen bonds n_{HB} in Table 1, it becomes clear that a non-uniform accumulation of water molecules around the ectoines is mainly induced by the carboxylic group (R1).

By the analysis of these properties, we have shown that a stronger hygroscopic effect is mainly induced by the presence of zwitterionic groups compared to urea. Additionally the size of the molecule is of importance due to the total solvent accessible surface area in contrast to the ratio of the hydrophilic surface area. Thus the pure static properties imply an advantage of the ectoines over urea which is less able to bind water molecules. Hence water capturing at dry situations is better achieved by the extremolytes in agreement to their biological function.

The results for the radial distribution function of water molecules around the center of mass for the compatible solutes are presented in Fig. 3. Hydroxyectoine and ectoine have nearly identical distribution functions with pronounced peaks at 0.5 nm (hydroxyectoine) and 0.54 nm (ectoine). Urea shows two peaks at 0.24 nm and 0.4 nm. This can be explained by the size of urea which allows the water molecules to form a hydration sphere on a smaller length scale. The influence on the molecular water structure decays around 1 nm to reach the bulk value for all molecules. Hence the main influence of the compatible solutes on the water molecules is located within this distance.

A more detailed investigation of the water binding to the functional groups has been also performed (data not shown). The carboxylic group

Table 1
Hydrophilic surface σ_h and its ratio r_σ to the total surface area, number of hydrogen bonds n_{HB}, net number of hydrogen bonds n_{HB}^c and average hydrogen bond density ρ_{HB}.

Molecule	Urea	Ectoine	Hydroxyectoine
σ_h [nm^2]	1.41 ± 0.01	1.63 ± 0.01	1.73 ± 0.01
r_σ	1	0.64 ± 0.01	0.67 ± 0.01
n_{HB}	4.43	7.01	8.77
n_{HB}^c	3.35	6.31	7.75
ρ_{HB} [nm^{-2}]	3.14 ± 0.03	2.75 ± 0.01	3.39 ± 0.02

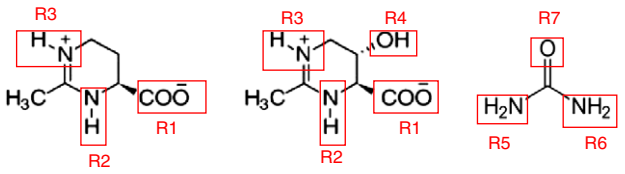

Fig. 2. Polar groups in ectoine (left), hydroxyectoine (middle) and urea (right).

R1 is able to form a pronounced structuring of the water molecules around distances 0.22 and 0.34 nm. The main contribution at 0.54 nm for ectoine and 0.5 nm for hydroxyectoine as it was shown in Fig. 3 is related to the effect of all contributing functional groups. Hence at these distances all polar groups are able to bind water molecules which yield a concerted contribution to the radial distribution function resulting in the peaks presented in Fig. 3. Additionally it can be shown that the large peak for urea at 0.2 nm is mainly caused by the presence of oxygen (R7). Thus it can be concluded that all studied molecules are able to form a pronounced accumulation sphere of water molecules at short distances. With these results we are able to indicate the length scale of the most significant interactions. As it has been discussed in Refs. [21,26], extremolytes interact with macromolecules via solvent mediated effects. Hence relevant interactions have to be taken place within this distance.

The results for the radial distribution function are in good agreement to the results for the local pressure of the water molecules around the compatible solutes shown in Fig. 4 which was calculated by the method proposed in Ref. [46]. In general the values for the pressure are mainly dominated by interparticle forces. It can be shown [46] that the pressure tensor $p_{\alpha\beta}(r)$ depends on $p_{\alpha\beta}(r) \sim F_{ij,\alpha} r_{ij,\beta}$ where F_{ij} denotes the conservative interparticle force and r_{ij} the distance between the particles i and j along the directions α and β. Hence it is obvious, that negative parts of the pressure correspond to attractive forces of the water molecules towards the center of the compatible solutes and positive values can be related to repulsive interactions. Large negative values can be observed for urea on distances up to 0.45 nm indicating strong attractive interactions. Hydroxyectoine and ectoine have negative values on distances up to 0.55 and 0.6 nm, respectively. It is obvious that the local pressure on scales 0.45–0.55 nm is drastically decreased in presence of ectoine. Additionally it can be seen that hydroxyectoine has a direct influence on the local solvent pressure by a large reduction on scales 0.425 to 0.525 nm. Hence, it can be concluded that water molecules are strongly correlated with the compatible solutes on short length scales which is significantly indicated by the discussed negative values. It is obvious that these results are in good agreement to Fig. 3 although a detailed analytical derivation is complicated [44]. Additionally we have calculated the pressure differences between charged and uncharged compatible solutes. It comes out that the differences additionally show an attractive net interaction between the compatible solutes and the water molecules as presented in the Supplementary material. It can be assumed that in the presence of a protein or a monolayer, the strong interaction towards the center of the compatible solutes causes a significant contribution on the hydration shell of the macromolecule which can be additionally responsible for the preservation of the native state. This is in particular important for distances between the compatible solute and the protein which are smaller than 0.7 nm as they have been reported in Ref. [21].

Table 2
Average hydrogen bonds and average lifetime per functional group (in brackets) per molecule.

Group	Ectoine	Hydroxyectoine	Urea
R1	5.59 (11.99 ps)	5.26 (13.08 ps)	–
R2	0.68 (5.81 ps)	0.84 (7.78 ps)	–
R3	0.75 (6.89 ps)	0.69 (6.32 ps)	–
R4	–	1.98 (9.89 ps)	–
R5	–	–	0.90 (5.24 ps)
R6	–	–	0.83 (5.35 ps)
R7	–	–	2.71 (13.40 ps)

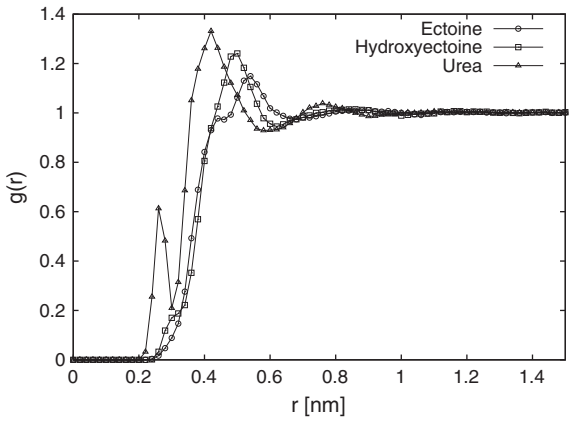

Fig. 3. Radial distribution function $g(r)$ for water molecules around the compatible solutes ectoine, hydroxyectoine and urea.

For a further discussion, we analyzed the relevant length scales for all molecules which can be related to different types of interactions. Very short distances which are smaller than 0.4 nm may correspond to direct interactions like hydrogen bonds. In addition, on a longer length scale r>0.8 nm only small variations can be observed in Fig. 4. Hence it can be again concluded that the relevant length scale $r = 0.4-0.6$ nm is the most important one for the influence of compatible solutes on other molecules as it has been mentioned in the introduction and in Ref. [21]. The drastic influence on the local water pressure in the important interval $r = 0.4-0.6$ nm is obvious. Hydroxyectoine has an average pressure of −4200 bar, ectoine a value of −3200 bar and urea a positive value of 550.

The effect of water accumulation can be also considered by calculating the radial cumulative number distribution function after Eq. (2). For a comparison, we conducted simulations with uncharged compatible solutes by setting all partial charges to zero. The results for the distribution function derived by these simulations are used to define a reference system which aims to investigate the influence of the atomic charges.

Our findings for the differences of the radial cumulative number distribution function $\Delta f(r)$ are shown in Fig. 5. It is evident that hydroxyectoine is able to bind up to nine water molecules, respectively seven water molecules for ectoine on a distance smaller than 0.5 nm. Urea binds approximately three molecules on a distance r<0.4 nm. These results are closely related to the average number of hydrogen bonds displayed in Table 2 and are in agreement to the hygroscopic characteristics

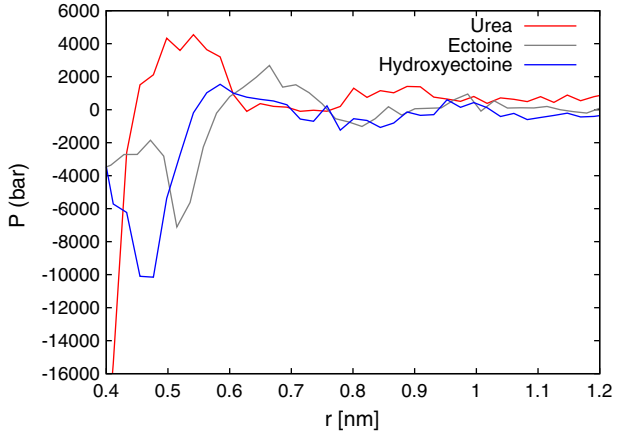

Fig. 4. Pressure in the bulk water phase around the compatible solutes.

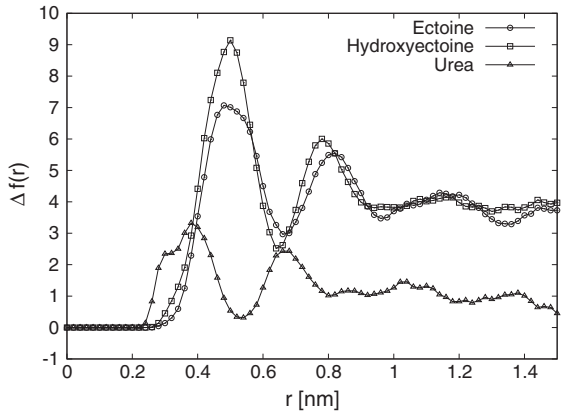

Fig. 5. Difference of the radial cumulative number distribution function $\Delta f(r)$ for water molecules around the compatible solutes.

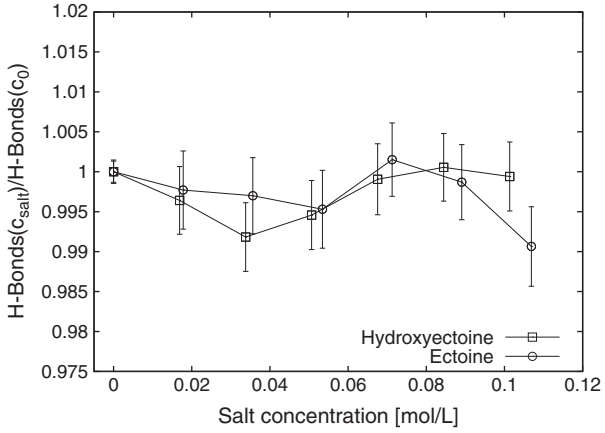

Fig. 6. Number of hydrogen bonds in presence of salt divided by the average values without salt given in Table 1.

of the molecules. The larger values for hydroxyectoine in contrast to ectoine are caused by the hydroxyl group (R4) which is able to bind nearly two water molecules (Table 2). However, a significant effect can be observed on distances larger than 1 nm. The net value for accumulated water is given by approximately four molecules for the ectoines and one for urea. Hydrogen bonding is not present at these distances which indicates that these water molecules are effectively accumulated due to indirect ordering and electrostatic effects. Thus the indirect long range influence of extremolytes on the local water structure is obvious. We conclude from these data that extremolytes are able to significantly change the local water environment. Due to the analysis of the relevant length scales, one can assume that these perturbations are mainly responsible for the preservation mechanism of macromolecules.

4.1. Influence of a varying salt concentration

Another interesting quantity is the direct influence of salt on the hygroscopic properties of the solutes. As it was mentioned in the introduction, extremolytes allow the cell to resist high salinity. Therefore we expect the influence of salt to be negligible for the properties of the extremolytes.

To investigate this point in more detail, we simulated salt solutions with concentration values ranging from 0.017 mol/L to 0.47 mol/L which is comparable to experimental and physiological conditions [1]. As it can be concluded from the data shown above, main indicators for deliquescent properties are large numbers of apparent hydrogen bonds.

Therefore we have compared the number of hydrogen bonds for an increasing salt concentration to the ratio of the values for the zero salt simulations given in Table 1. The results are shown in Fig. 6.

The ratio is always above 0.98, which is also true for salt concentrations of 0.47 mol/L (data not shown) which indicates a minor influence of salt on the number of hydrogen bonds. Therefore it can be concluded that high salinity does not affect the hygroscopic properties of extremolytes. This implies that the extremolytes are able to bind water molecules even under harsh conditions which allows to protect the cell against drying out.

4.2. Effects of compatible solutes on the structural organization of DPPC monolayers

As we have mentioned in the introduction an important impact of extremolytes on biomolecular assemblies is to increase the fluidity of membranes under specific circumstances [25,26]. Regions with increased flexibility are included in the liquid expanded (LE) phase whereas more rigid domains are given in the liquid condensed (LC) phase.

In a lipid monolayer the formation of several domains can be experimentally observed under certain temperature conditions in coexistence of the LE phase [47,48]. A driving force to understand the formation of these regions has been indicated to be the line tension [49,50].

Fluid phase coexistence in lipid membranes is characterized by the formation of both LC phase as well as the LE phase. The LC phase exhibits a higher degree of ordering and packing preventing water to penetrate the hydrophobic core. Hence the mechanical elasticity is increased in the LE phase. It has been shown [25] that the presence of hydroxyectoine and ectoine modifies the formation of the LC domains and therefore ensures the fluidization of the monolayer. This effect has been described by a variation of the preferential exclusion model [13–15,20,21,25] as well as a direct influence of the extremolytes on the lipid headgroup region [26].

We have carried out experiments for a DPPC monolayer in presence of the different compatible solutes hydroxyectoine, ectoine and urea to investigate the influence of each species on the LE/LC phase transition. Due to the relative ordering of the molecules by their hygroscopic properties, we expect the phase transition to reflect this behavior.

The fluorescence pictures of the monolayers doped with BODIPY-PC, a fluorescent dye that is preferentially soluble in the fluid LE phase are shown in Fig. 7. Dark domains represent the rigid LC phase, light areas the more fluid LE phase. Lipid films on pure water exhibit the well known kidney shaped LC domains in the phase transition region [25]. The extent of the LC phase increases for all molecules with increasing surface pressure.

In pure water the characteristic multi-lobed structure starts to form at 5 mN/m and is fully pronounced at 7 mN/m as a left-handed clearly developed nanostructure. The presence of urea is only important at 7 mN/m where the domain size is considerably decreased in comparison to the results of pure water. No visible effect can be observed at 5 mN/m.

Ectoine at 5 mN/m leads to a considerable shrinkage in the domain size. At both 5 mN/m and 7 mN/m the well developed domain structure is therefore lost continuously. This effect is even more enhanced for a solution containing hydroxyectoine.

Thus it is obvious that hydroxyectoine and ectoine have a more distinct effect than urea on DPPC monolayers which is in accordance to the numerical results shown above. It can be assumed that the effects appear on a length scale larger than 0.4 nm [21] in front of the macromolecular surface which sheds a new light on the second order packing structures indicated by Fig. 5.

As it is obvious and discussed above, the extremolytes have a net effect on long and short distances on the solvent configuration. It can be concluded that the specific alteration of the solvent environment as indicated by the results shown above is directly reflected in the

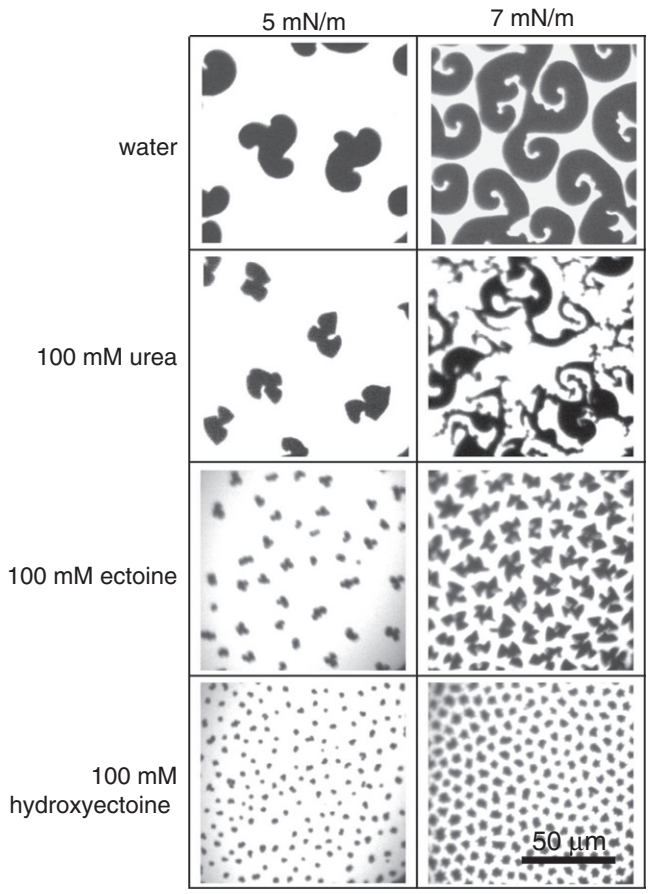

Fig. 7. Video-enhanced fluorescence microscopic images of DPPC monolayers on subphases containing ectoine, hydroxyectoine and urea. All measurements were performed at 20 °C and surface pressures 5 (left) and 7 mN/m (right). The results for hydroxyectoine and ectoine have been taken from [25] for the ease of comparison.

broadening of the monolayer phase transition. Hence the experimental results validate the relative ordering of the compatible solutes related to their hygroscopic characteristics. These results are also in good agreement to the observed surface pressure isotherms that are presented in the supplementary material.

5. Summary and conclusion

We have investigated the microscopic deliquescent properties of the compatible solutes and their influence on the local water structure. Our results indicate that ectoine and hydroxyectoine are able to bind more water molecules than urea. Thus the usage of extremolytes as water binding chemical detergents in dermatologic products is validated. By comparison to the uncharged, purely steric interacting species we found that the extremolytes are able to accumulate nine and seven water molecules for hydroxyectoine and ectoine, respectively, in a distance located within 0.6 nm. The reason for this behavior is the formation of a large number of hydrogen bonds at specific functional groups of the molecules.

Furthermore we have determined a net value of four accumulated water molecules for the extremolytes on length scales larger than 0.6 nm. This value can be related to second order packing effects due to the fact that direct interactions like hydrogen bonds are absent on these distances.

Although the extremolytes are charged and act via electrostatic interactions with the solvent, we have shown that the presence of salt does only slightly alter the number of hydrogen bonds. Hence, the specific water binding behavior of the compatible solutes is not perturbed at high salt concentrations. Compared to urea, ectoine and hydroxyectoine have more distinct hygroscopic properties. One can therefore identify extremolytes as water-binding molecules which order the local structure of the solvent on a length scale of 0.6 nm significantly. On longer length scales second order effects can be observed which result in net water accumulation due to packing effects.

Finally we experimentally studied the impact of the compatible solutes on the formation of domains in the LE–LC phase transition of lipid monolayers. Our results indicate that ectoine and hydroxyectoine broaden the phase transition by suppressing the appearance of LC domains. Thus the mechanical flexibility of the monolayer is more enhanced in the presence of extremolytes compared to urea. These results can be brought into accordance to the numerical data concerning the relative hygroscopicity and the long range ordering effects of the local water structure.

Summarizing all results, our study has shown that the hygroscopic properties of several compatible solutes significantly differ in their specific behavior. Our findings allow to achieve a more detailed view on the structural alteration of the local water environment. As it has been discussed in the introduction, the stabilizing effect of co-solvent on proteins and lipid monolayer has been studied in detail before. However, a theoretical investigation concerning the important length scales has been missing.

We have shown that the relevant distances between interacting species which have been found in the literature at 0.4–0.6 nm [21] are validated by a significant modification of the water ordering. Hence, our results allow to conclude that this distance is naturally implied by the effects of solvent ordering. Although we have neglected the presence of target molecules, our results indicate the large hygroscopicity of the ectoines as a main reason for the preservation mechanism. Due to the zwitterionic properties and the hydrophobic/hydrophilic surface area contributions, the ectoines are repelled from a proteins surface such that the deliquescent characteristics lead to a strong binding of water molecules. It can be assumed that some parts of these processes are mainly involved in the stabilization mechanism.

Due to the actual large number of hydrogen bonds even in high salt concentrations, we have validated that a significant increase of ions does not change the molecular properties. Electrostatic screening of the zwitterionic parts can be neglected such that the functionality of the co-solvents is conserved even under harsh conditions. Thus, we have validated that the ectoines are a specific class of molecules which significantly differ from other osmolytes due to their hygroscopic characteristics and the variation of the water environment. Strong binding of solvent molecules indicates them as perfect molecules against drying out. The evolutionary strategy to overcome dry situations for microorganisms by the synthesis of extremolytes is supported by our data. All our results indicate that ectoine and hydroxyectoine are better suited as hygroscopic detergents in dermatological products than long known hygroscopic molecules like urea.

Acknowledgments

Financial support by the Deutsche Forschungsgemeinschaft (DFG) through the transregional collaborative research center TRR 61 and the SFB 858 is gratefully acknowledged. R. K. Harishchandra acknowledges funding from the International Graduate School in Chemistry at the University of Münster. Additional results can be found in the supplementary material.

Appendix A. Supplementary data

Supplementary data to this article can be found online at doi:10.1016/j.bpc.2011.09.007.

References

[1] G. Lentzen, T. Schwarz, Extremolytes: natural compounds from extremophiles for versatile applications, Appl. Microbiol. Biotechnol. 72 (2006) 623–634.
[2] R. Graf, S. Anzali, J. Buenger, F. Pfluecker, H. Driller, The multifunctional role of ectoine as a natural cell protectant, Clin. Dermatol. 26 (2008) 326–333.
[3] A.D. Brown, Compatible solutes and extreme water stress in eukaryotic microorganisms, Adv. Microb. Physiol. 17 (1978) 181–242.
[4] E.A. Galinski, H.P. Pfeiffer, H.G. Truper, 1,4,5,6-Tetrahydro-2-methyl-4-pyrimidinecarboxylic acid: a novel cyclic amino acid from halophilic phototrophic bacteria of the genus *Ectothiorhodospira*, Eur. J. Biochem. 149 (1985) 135–139.
[5] E.A. Galinski, Compatible solutes of halophilic eubacteria: molecular principles, water–solute interactions, stress protection, Experientia 49 (1993) 487–496.
[6] L. Inbar, A. Lapidot, The structure and biosynthesis of new tetrahydropyrimidine derivatives in actinomycin D producer Streptomyces parvulus. Use of ^{13}C- and ^{15}N-labeled L-glutamate and ^{13}C and ^{15}N NMR spectroscopy, J. Biol. Chem. 263 (1988) 16014–16022.
[7] W. Schuh, H. Puff, E.A. Galinski, H.G. Truper, The crystal structure of ectoine, a novel amino acid of potential osmoregulatory function, Z. Naturforsch. 40c (1985) 780–784.
[8] L. Inbar, F. Frolow, A. Lapidot, The conformation of new tetrahydropyrimidine derivatives in solution and in the crystal, Eur. J. Biochem. 214 (1993) 897–906.
[9] K. Suenobu, M. Nagaoka, T. Yamabe, S. Nagata, Ab initio molecular orbital study on molecular and hydration structures of ectoine, J. Phys. Chem. A 102 (1998) 7505–7511.
[10] T. Dirschka, Ectoin-use and perspectives for dermatology, Akt. Dermatol. 34 (2008) 115–118.
[11] P. Lamosa, D.L. Turner, R. Ventura, C. Maycock, H. Santos, Protein stabilization by compatible solutes. Effect of diglycerol phosphate on the dynamics of Desulfovibrio gigas rubredoxin studied by NMR, Eur. J. Biochem. 270 (2003) 4606–4616.
[12] R.L. Foord, R.J. Leatherbarrow, Effect of osmolytes on the exchange rates of backbone amide protons in proteins, Biochemistry 37 (1998) 2969–2978.
[13] C.J. Lee, S.N. Timasheff, The stabilization of proteins by sucrose, J. Biol. Chem. 256 (1981) 7193–7201.
[14] T. Arakawa, S.N. Timasheff, Preferential interactions of proteins with solvent components in aqueous amino acid solutions, Arch. Biochem. Biophys. 224 (1983) 169–177.
[15] T. Arakawa, S.N. Timasheff, The stabilization of proteins by osmolytes, Biophys. J. 47 (1985) 411–414.
[16] S.N. Timasheff, Protein hydration, thermodynamic binding, and preferential hydration, Biochemistry 41 (2002) 13473–13482.
[17] T.O. Street, D.W. Bolen, G.D. Rose, A molecular mechanism for osmolyte-induced stability, Proc Natl. Acad. Sci. 103 (2006) 13997–14002.
[18] D.W. Bolen, G.D. Rose, Structure and energetics of the hydrogen-bonded backbone in protein folding, Annu. Rev. Biochem. 77 (2008) 339–362.
[19] J.A. Schellman, Protein stability in mixed solvents: a balance of contact interaction and excluded volume, Biophys. J. 85 (2003) 108–125.
[20] I. Yu, M. Nagaoka, Slowdown of water diffusion around protein in aqueous solution with ectoine, Chem. Phys. Lett. 388 (2004) 316–321.
[21] I. Yu, Y. Jindo, M. Nagaoka, Microscopic understanding of preferential exclusion of compatible solute ectoine: direct interaction and hydration alteration, J. Phys. Chem. B 111 (2007) 10231–10238.
[22] S. Knapp, R. Ladenstein, E.A. Galinski, Extrinsic protein stabilization by the naturally occurring osmolytes beta-hydroxyectoine and betaine, Extremophiles 3 (1999) 191–198.
[23] P.H. Yancey, M.E. Clark, S.C. Hand, R.D. Bowlus, G.N. Somero, Living with water stress: evolution of osmolyte systems, Science 217 (1982) 1214–1222.
[24] C. Held, T. Neuhaus, G. Sadowski, Compatible solutes: thermodynamic properties and biological impact of ectoines and prolines, Biophys. Chem. 152 (2010) 28–39.
[25] R.K. Harishchandra, S. Wulff, G. Lentzen, T. Neuhaus, H.-J. Galla, The effect of compatible solute ectoines on the structural organization of lipid monolayer and bilayer membranes, Biophys. Chem. 150 (2010) 37–46.
[26] R.K. Harishchandra, A.K. Sachan, A. Kerth, G. Lentzen, T. Neuhaus, H.-J. Galla, Compatible solutes: Ectoine and hydroxyectoine improve functional nanostructures in artificial lung surfactants, BBA-Biomembranes (2011), doi:10.1016/j.bbamem.606 2011.02.022.
[27] J. Bünger, J. Degwert, H. Driller, The protective function of compatible solute ectoin on the skin, skin cells and its biomolecules with respect to UV radiation, immunosuppression and membrane damage, IFSCC Mag. 4 (2001) 127–131.
[28] H.J.C. Berendsen, J.R. Grigera, T.P. Straatsma, The missing term in effective pair potentials, J. Phys. Chem. 91 (1987) 6269–6271.
[29] H.J.C. Berendsen, D. van der Spoel, R. van Drunen, GROMACS: a message-passing parallel molecular dynamics implementation, Comp. Phys. Comm. 91 (1995) 43–56.
[30] B. Hess, C. Kutzner, D. van der Spoel, E. Lindahl, GROMACS 4: algorithms for highly efficient, load-balanced, and scalable molecular simulation, J. Chem. Theory Comput. 4 (2008) 435–447.
[31] D. Van der Spoel, E. Lindahl, B. Hess, G. Groenhof, A.E. Mark, H.J.C. Berendsen, Gromacs: fast, flexible and free, J. Comp. Chem. 26 (2005) 1701–1718.
[32] C. Oostenbrink, A. Villa, A.E. Mark, W.F. van Gunsteren, A biomolecular force field based on the free enthalpy of hydration and solvation: the GROMOS force-field parameter sets 53A5 and 53A6, J. Comp. Chem. 25 (2004) 1656–1676.
[33] D. Weininger, SMILES, a chemical language and information system. 1. Introduction to methodology and encoding rules, J. Chem. Inf. Comput. Sci. 28 (1988) 31–36.
[34] http://cactus.nci.nih.gov/services/translate/(accessed September 19th, 2011).
[35] A.W. Schüttelkopf, D.M.F. van Aalten, PRODRG: a tool for high-throughput crystallography of protein–ligand complexes, Acta Cryst. D60 (2004) 1355–1363.
[36] R. Ahlrichs, M. Bär, M. Häser, M. Horn, C. Kölmel, Electronic structure calculations on workstation computers: the program system turbomole, Chem. Phys. Lett. 162 (1989) 165–169.
[37] F. Weigend, M. Häser, H. Patzelt, R. Ahlrichs, RI-MP2: optimized auxiliary basis sets and demonstration of efficiency, Chem. Phys. Lett. 294 (1998) 143–152.
[38] C. Haettig, Optimization of auxiliary basis sets for RI-MP2 and RI-CC2 calculations: corevalence and quintuple-basis sets for H to Ar and QZVPP basis sets for Li to Kr, Phys. Chem. Chem. Phys. 7 (2005) 59–66.
[39] A. Schäfer, A. Klamt, D. Sattel, J.W.C. Lohrenz, F. Eckert, COSMO implementation in TURBOMOLE: extension of an efficient quantum chemical code towards liquid systems, Phys. Chem. Chem. Phys. 2 (2000) 2187–2193.
[40] A. Klamt, G. Schüürmann, COSMO: a new approach to dielectric screening in solvents with explicit expressions for the screening energy and its gradient, J. Chem. Soc. Perkin Trans. 2 (1993) 799–805.
[41] U. Essman, L. Perela, M.L. Berkowitz, T. Darden, H. Lee, L.G. Pedersen, A smooth particle mesh Ewald method, J. Chem. Phys. 103 (1995) 8577–8593.
[42] D. Frenkel, B. Smit, Understanding Molecular Simulation, Academic Press, San Diego, 1996.
[43] B. Hess, H. Bekker, H.J.C. Berendsen, J.G.E.M. Fraaije, LINCS: a linear constraint solver for molecular simulations, J. Comp. Chem. 18 (1997) 1463–1472.
[44] M.P. Allen, D.J. Tildesley, Computer simulation of liquids, Oxford Science Publications, Oxford, 1987.
[45] F. Eisenhaber, P. Lijnzaad, P. Argos, C. Sander, M. Scharf, The double cubic lattice method: efficient approaches to numerical integration of surface area and volume and to dot surface contouring of molecular assemblies, J. Comp. Chem. 16 (1995) 273–284.
[46] O.H.S. Ollila, H.J. Risselada, M. Louhivuori, E. Lindahl, I. Vattulainen, S.J. Marrink, 3D Pressure field in lipid membranes and membrane–protein complexes, Phys. Rev. Lett. 102 (2009) 0781011–0781015.
[47] C.W. McConlogue, T.K. Vanderlick, A close look at domain formation in DPPC monolayers, Langmuir 13 (1997) 7158–7164.
[48] P.E. Milhiet, M.-C. Giocondi, C. Le Grimellec, AFM imaging of lipid domains in model membranes, Sci. World J. 3 (2003) 59–74.
[49] D.J. Benvegnu, H.M. McConnell, Line tension between liquid domains in lipid monolayers, J. Phys. Chem. 96 (1992) 6820–6824.
[50] S. May, A molecular model for the line tension of lipid membranes, Eur. Phys. J. E. 3 (2000) 37–44.